

# Encoding of Spatially Coupled LDGM Codes for Lossy Source Compression

Ahmad Golmohammadi<sup>1</sup>, Student Member, IEEE, David G. M. Mitchell<sup>2</sup>, Senior Member, IEEE, Jörg Kliewer<sup>3</sup>, Senior Member, IEEE, and Daniel J. Costello, Jr., Life Fellow, IEEE

**Abstract**—It has been shown that a class of spatially coupled low-density generator-matrix (SC-LDGM) code ensembles displays distortion saturation for the lossy binary symmetric source coding problem with the belief propagation guided decimation (BPGD) algorithm, i.e., the BPGD distortion approaches the optimal expected distortion of the underlying ensemble asymptotically in code length. We investigate the distortion performance of a practical class of protograph-based SC-LDGM code ensembles and demonstrate distortion saturation numerically. Moreover, taking advantage of the convolutional structure of the SC-LDGM codes, we propose an efficient windowed encoding (WE) algorithm with two decimation techniques for lowering the WE complexity that maintain distortion performance close to the rate-distortion bound.

**Index Terms**—Lossy source coding, spatial coupling, LDGM codes, belief propagation guided decimation, rate distortion bound.

## I. INTRODUCTION

COMPARED to lossless compression, where the source must be reconstructed identically from its compressed version, the lossy source compression problem requires the reconstructed data to be correct only up to some specified distortion measure. Applying linear codes for lossy source compression of discrete sources is a classical idea [1], and various bounds on distortion performance have been proposed for different types of linear codes, e.g., trellis codes [2], [3], turbo-codes [4], LDPC codes [5], and polar codes [6]–[8]. Excellent reconstruction performance can be obtained with such approaches. For example, polar codes were shown to have optimal lossy source coding performance for the binary

symmetric source [8], and it was shown that it is possible to approach the binary rate-distortion (RD) limit using LDPC codes if the node degrees of the ensemble grow logarithmically with the block length [5]. Moreover, compound LDPC and low-density generator matrix (LDGM) codes have been shown to achieve the RD limit with bounded node degrees [9].

Low-density generator matrix block codes (LDGM-BCs), the duals of LDPC block codes (LDPC-BCs), were shown to achieve the RD limit under optimal encoding as the average node degrees increase [10], and lower bounds on the distortion have been derived both for random ensembles [11] and for specific code constructions [12]. Like LDPC-BCs, LDGM-BCs can be defined on a sparse graph and are amenable to low complexity message passing algorithms. Unfortunately, this approach typically fails because the lossy source coding problem has multiple optimal (or near-optimal) solutions and one cannot find the relevant fixed point without reducing the solution space. Heuristic decimation algorithms based on belief propagation (BP) [10], [13]–[15] and survey propagation [10], [16]–[18] have been proposed for lossy data compression for both linear and non-linear codes and have been successfully applied to  $k$ -satisfiability ( $k$ -SAT) constraint problems [13], [19], [20]. Also, good LDGM-BCs have been designed for the binary erasure source [21]–[23]; however, to the best of our knowledge, there have been no constructive LDGM-BC designs proposed with performance guarantees for general binary discrete sources. Indeed, the best known code designs are heuristic in nature and typically use dual codes to LDPC-BCs that were optimized for the binary symmetric channel (see, e.g., [10], [24], [25]).

Spatially coupled LDGM (SC-LDGM) codes can be obtained by coupling together (connecting) a series of  $L$  LDGM-BC graphs to make a larger connected graph with a convolutional-like structure. In [26] and [27], a belief propagation guided decimation (BPGD) algorithm was applied for lossy source compression of the binary symmetric source to a class of SC-LDGM codes with regular check node degrees and both Poisson distributed [26] and regular [27] variable node degrees. It was demonstrated there that the SC-LDGM code ensembles achieve distortion saturation, in the sense that the distortion of the SC-LDGM code ensemble approaches the optimal distortion for the underlying LDGM-BC ensemble as the coupling length and code length tend to infinity, which, in turn, approaches the RD limit as the node degrees increase. As a result, SC-LDGM codes have great promise for the lossy

Manuscript received December 8, 2017; revised April 22, 2018; accepted June 6, 2018. Date of publication June 18, 2018; date of current version November 16, 2018. This material is based upon work supported by the National Science Foundation under Grant Nos. CCF-1440001, CCF-1440001, and ECCS-1711056. This paper was presented in part at the 2016 IEEE International Symposium on Information Theory and in part at the 2016 IEEE International Symposium on Information Theory and Its Applications. The associate editor coordinating the review of this paper and approving it for publication was A. Thangaraj. (Corresponding author: Ahmad Golmohammadi.)

A. Golmohammadi and D. G. M. Mitchell are with the Klipsch School of Electrical and Computer Engineering, New Mexico State University, Las Cruces, NM 88003 USA (e-mail: golmoham@nmsu.edu; dgmm@nmsu.edu).

J. Kliewer is with the Department of Electrical and Computer Engineering, New Jersey Institute of Technology, Newark, NJ 07102 USA (e-mail: jkliewer@njit.edu).

D. J. Costello, Jr., is with the Department of Electrical Engineering, University of Notre Dame, Notre Dame, IN 46556 USA (e-mail: costello.2@nd.edu).

Color versions of one or more of the figures in this paper are available online at <http://ieeexplore.ieee.org>.

Digital Object Identifier 10.1109/TCOMM.2018.2848241

source coding problem, but the large code lengths required for distortion saturation with the standard BPGD algorithm make them unattractive in practice.

Motivated by the theoretical results of [26] and [27], this paper investigates several fundamental practical issues related to SC-LDGM codes. In particular, the main contributions are as follows:

- 1) We present a practically interesting  $(J, K)$ -regular SC-LDGM code construction based on *protographs*, which are amenable to efficient implementation (see, e.g., [28]). We demonstrate distortion saturation numerically for these protograph-based code ensembles and show that this effect is the result of a “wave-like” encoding behavior. Note that, even for the well studied SC-LDPC channel coding problem, it has not been proven that protograph-based SC-LDPC codes achieve threshold saturation and channel capacity. Thus demonstrating that practically interesting protograph-based SC-LDGM codes empirically achieve distortion saturation is a valuable result;
- 2) To reduce the latency and thus combat the need for very long code lengths, as is desirable in practice, we propose a novel windowed encoding (WE) scheme and demonstrate distortion performance close to the RD limit with moderate encoding latency for the binary symmetric source. To the best of our knowledge, regular SC-LDGM codes with the proposed WE scheme are the first regular LDGM constructions that perform close to the RD limit with low complexity encoding and moderate latency;
- 3) We propose a combined soft and hard decimation algorithm that allows the wave-like encoding to progress through the chain and reduces the average distortion compared to soft only decimation algorithms. Moreover, we present two further decimation approaches for WE that can significantly lower computational complexity (measured as the number of node updates). The first decimates a fixed number of nodes per iteration and the second decimates all nodes with sufficiently large confidence at each iteration. For both approaches, we study the trade-offs in terms of performance vs. complexity and show that the complexity can be significantly decreased with little loss in performance compared to decimating a single node per iteration;
- 4) We discuss the latency, complexity, and performance trade-offs of WE and compare the results with an optimized irregular LDGM-BC. Moreover, we demonstrate that a min-sum formulation can be used during the BP updates that further reduces the complexity at the cost of a slight loss in performance;
- 5) Finally, we demonstrate robust performance over a variety of compression rates for different  $(J, K)$ -regular SC-LDGM codes. Since there are many parameters involved in the code construction and encoding algorithms, one of our goals is to explain their effect on performance with respect to the distortion/latency/complexity trade-offs and to give a system

designer guidance in choosing reasonable parameter sets for implementation.

The remainder of the paper is organized as follows. Section II contains necessary background material on lossy source coding and introduces protograph-based SC-LDGM codes. In Section III, the proposed source compression algorithm for SC-LDGM codes is presented along with experimental results showing distortion saturation and a discussion of the wave-like encoding behavior. In Section IV, we present the windowed encoding algorithms, including a study of the distortion/latency/complexity trade-offs. We conclude the paper in Section V.

## II. SC-LDGM CODE ENSEMBLES FOR LOSSY COMPRESSION

### A. Lossy Source Compression

In this paper, we consider compressing the *symmetric Bernoulli source* [29], where the source sequence  $\mathbf{s} = (s_1, s_2, \dots, s_n) \in F_2^n$  consists of independent and identically distributed (i.i.d.) random variables with  $\mathbb{P}(s_i = 1) = 1/2$ ,  $i = 1, 2, \dots, n$ . We wish to represent a given source sequence by some codeword  $\mathbf{z} \in F_2^m$  from a given code  $C$  containing  $2^m = 2^{nR}$  codewords, where  $m \ll n$  and  $R = \frac{m}{n}$  is the *compression rate*. The codeword  $\mathbf{z}$  is used to reconstruct the source sequence as  $\hat{\mathbf{s}}$ , where the mapping  $\mathbf{z} \rightarrow \hat{\mathbf{s}}(\mathbf{z})$  depends on the code  $C$ . The quality of reconstruction is measured by a *distortion metric*  $d : \mathbf{s} \times \hat{\mathbf{s}} \rightarrow \mathbf{R}^+$  and the resulting source encoding problem is to find the codeword with minimal distortion, i.e.,  $\hat{\mathbf{z}} = \arg \min_{\mathbf{z}} d(\mathbf{s}, \hat{\mathbf{s}})$ . For a symmetric Bernoulli source, the typical measure of distortion is the *Hamming metric*  $d_H(\mathbf{s}, \hat{\mathbf{s}}) = \frac{1}{n} \sum_{i=1}^n |s_i - \hat{s}_i|$ , and thus the average quality of the reconstruction is measured as  $\bar{D} = \mathbb{E}_{\mathbf{s}}[d_H(\mathbf{s}, \hat{\mathbf{s}})]$ . For any encoding scheme, the average distortion is bounded below by *Shannon's RD limit*  $D_{Sh}$ , defined implicitly by the rate-distortion function  $h(D_{Sh}) = 1 - R$ ,  $D_{Sh} \in [0, 0.5]$ , where  $h(\cdot)$  is the binary entropy function [30]. The goal is to find an encoding scheme that achieves the rate-distortion bound for a given  $R$ .

### B. Protograph-Based SC-LDGM Codes

An LDGM-BC ensemble can be represented by means of a *protograph* [31], a small bipartite graph that connects a set of  $n$  source (information) and  $m$  code (compressed) nodes to a set of  $n$  generator nodes by a set of edges. It can be represented by a generator or *base* biadjacency matrix  $\mathbf{B}$ , where  $B_{x,y}$  is taken to be the number of edges connecting generator node  $g_y$  to code node  $z_x$ . The generator matrix  $\mathbf{G}$  of a protograph-based LDGM-BC can then be created by expanding  $\mathbf{B}$  using a *lifting factor*  $M$ , where each non-zero entry in  $\mathbf{B}$  is replaced by a sum of  $B_{x,y}$  non-overlapping permutation matrices of size  $M \times M$  and each zero entry is replaced by the  $M \times M$  all-zero matrix. Fig. 1 depicts the protograph representation of a  $(3, 6)$ -regular LDGM-BC ensemble with the all-ones base matrix  $\mathbf{B}$  of size  $3 \times 6$ . The white and black circles represent source (information) and code (compressed) symbols, respectively. After compression, the reconstructed source symbols  $\hat{s}_i$  are obtained by a modulo 2 summation at the generator nodes.



### Code node bias update:

$$B_i^{(t)} = \tanh\left(\frac{R_i^{(t)}}{2}\right), \quad B_{i \rightarrow a}^{(t)} = \tanh\left(\frac{R_{i \rightarrow a}^{(t)}}{2}\right), \quad (6)$$

where  $R_{i \rightarrow a}^{(t)}$ ,  $R_{a \rightarrow i}^{(t)}$ , and  $B_{i \rightarrow a}^{(t)}$  denote the message sent from code node  $i$  to generator node  $a$ , the message sent from generator node  $a$  to code node  $i$ , and the bias associated with  $R_{i \rightarrow a}^{(t)}$  at iteration  $t$ , respectively, and  $\beta$  and  $\mu$  are parameters. Then  $R_i^{(t)}$  and  $B_i^{(t)}$  denote the likelihood ratio of code node  $i$  and the bias associated with  $R_i^{(t)}$ , respectively. Also, for an LDGM graph  $\Gamma$  with code nodes  $Z$  and generator nodes  $G$ ,  $Z(a)$  denotes the set of all code node indices connected to generator node  $a$ ,  $|Z(a)|$  is its cardinality, and  $G(i)$  denotes the set of all generator node indices connected to code node  $i$ ,  $\forall i \in Z$  and  $\forall a \in G$ . Without the term  $\frac{1}{\mu}R_{i \rightarrow a}^{(t)}$  in (5), equations (4)-(6) are equivalent to BP with no decimation. Including the first term in (5) incorporates soft-decimation via the “soft-indicator” function [25]  $I_{soft}(B_{i \rightarrow a}^{(t)}) = \frac{2}{\mu} \tanh^{-1}(B_{i \rightarrow a}^{(t)}) = \frac{1}{\mu}R_{i \rightarrow a}^{(t)}$ , which approximates the “hard-indicator” function

$$I_{hard}(B_{i \rightarrow a}^{(t)}) = \begin{cases} -\infty & B_{i \rightarrow a}^{(t)} = -1 \\ 0 & -1 < B_{i \rightarrow a}^{(t)} < 1, \\ +\infty & B_{i \rightarrow a}^{(t)} = 1 \end{cases} \quad (7)$$

where  $\mu$  controls the “softness” of the approximation. For further details, see [25]. Since  $\beta$  and  $\mu$  are free parameters, they can be optimized independently; however, here we choose them as  $\beta = (1 - \xi)/(1 + \xi)$  and  $\mu = 1/\xi$  for simplicity, where  $\xi$  is called the *tuning parameter*. This choice simplified the optimization and was shown to yield good numerical results in [25].

### B. Soft-Hard Decimation

The BP algorithm used in this paper is a mixture of both hard and soft decimation. The algorithm uses the soft decimation equations given above, but after each iteration it searches for a code node with maximum bias value. This code node is then decimated (permanently fixed) and the current graph reduced following the hard decimation rule. This modification is applied to force decimation to occur in designated areas of the code graph in order to take advantage of the convolutional structure of SC-LDGM codes. The procedure is described in detail as Algorithm A, where  $t$  indicates the iteration number,  $\Gamma^{(t)}$  is the LDGM code graph at iteration  $t$ , and  $z_i$  represents the binary value assigned to code node  $i$ . The initial code to generator node messages,  $R_{i \rightarrow a}^{(0)}$ , are set to  $\pm 0.1$  with  $\mathbb{P}(R_{i \rightarrow a}^{(0)} = 0.1) = 0.5$ , and reset to 0 at iteration 1.

### C. Analysis and Dynamics of Encoding SC-LDGM Codes

In this subsection, the results of various experiments of a C++-based implementation of Algorithm A are reported for different SC-LDGM code parameters. Codes were obtained by randomly lifting the protograph and all results were obtained by averaging over 1000 trials.

### Algorithm A Soft-Hard Decimation

- 1) At iteration  $t = 0$ , initialize graph instance  $\Gamma^{(t=0)}$
- 2) Update equations (4), (5), and (6)
- 3) Find the maximum bias  $B^{(t)} = \max_i \{|B_i^{(t)}| \mid i \text{ not fixed}\}$
- 4) **If**  $B^{(t)} > 0$  then
  - $z_i \leftarrow '1'$
  - else**
  - $z_i \leftarrow '0'$
- 5) Decimate graph as
  - a)  $\forall a \in G(i)$ ,  $s_a \leftarrow s_a \oplus z_i$  (update source symbols)
  - b) reduce the graph as  $\Gamma^{(t+1)} = \Gamma^{(t)} \setminus \{i\}$  (remove code node  $i$  and all its edges)
- 6) **If** there exist any unassigned code symbols  $z_i$  go to 2)
  - else**
  - exit algorithm and return code symbols

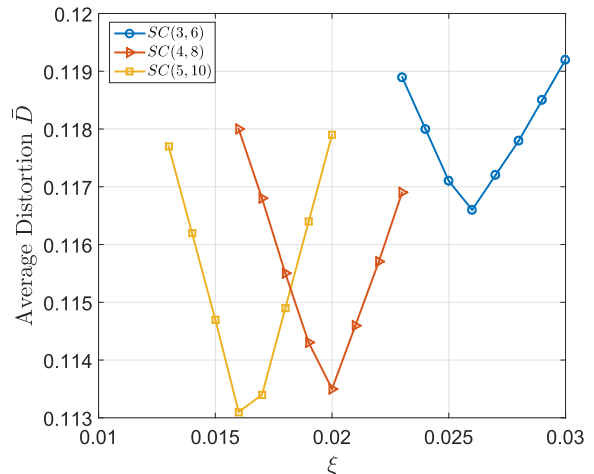


Fig. 3. The performance of Algorithm A as a function of  $\xi$  for SC(3, 6), SC(4, 8), and SC(5, 10) code with length  $n = 102400$ , coupling length  $L = 100$ , and compression rate  $R_L = 0.5050$ .

1) *Effect of the Tuning Parameter  $\xi$* : Fig. 3 shows the average distortion versus  $\xi$  for SC(3, 6), SC(4, 8), and SC(5, 10) codes with code length  $n = 102400$ , coupling length  $L = 100$ , and compression rate  $R_L = 0.5050$ . By running the proposed algorithm for SC(3, 6), SC(4, 8), and SC(5, 10) codes, choosing the (experimentally determined to three decimal places) optimum  $\xi$ , denoted  $\xi^*$ , and averaging over 1000 trials, average distortion values  $\bar{D} = 0.116609$ ,  $\bar{D} = 0.113463$ , and  $\bar{D} = 0.113137$  are obtained, respectively. Fig. 3 shows that the performance of the algorithm depends on the choice of  $\xi$ . We note that the optimum value of  $\xi$  for the SC(3, 6), SC(4, 8), and SC(5, 10) codes is different and that by increasing the encoder node degrees from 3 to 5, the optimum value of  $\xi$  decreases. Moreover, Fig. 3 indicates that the sensitivity of the algorithm with respect to  $\xi$ , *i.e.*, the sharpness of the minima, tends to increase with increasing density  $J$ .

2) *Effect of Increasing the Coupling Length  $L$* : We now consider SC-LDGM codes with fixed lifting factor  $M = 512$

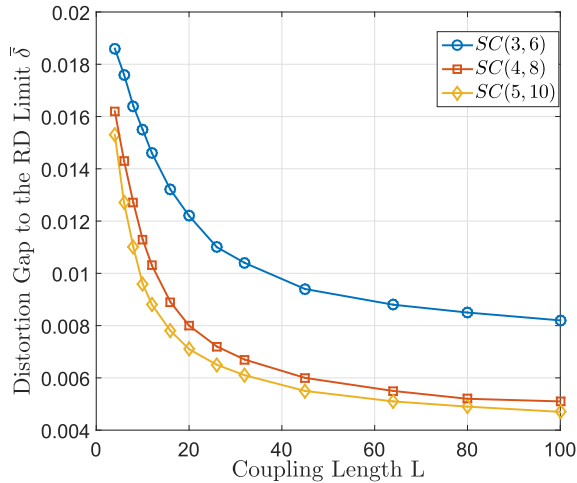


Fig. 4. Average distortion gap to the RD limit obtained for SC(3, 6), SC(4, 8), and SC(5, 10) codes with fixed  $M = 512$  and increasing  $L$ .

TABLE I

EFFECT OF THE LIFTING FACTOR  $M$  ON SC(4, 8) CODES IN TERMS OF AVERAGE DISTORTION  $\bar{D}$  AND AVERAGE GAP TO THE RD LIMIT  $\bar{\delta}$  WITH FIXED  $L = 16$  AND COMPRESSION RATE  $R_L = 0.5313$

Lifting factor ( $M$ )	$\bar{D}$	$\bar{\delta}$
128	0.112675	0.0128
192	0.110917	0.0110
256	0.110074	0.0102
320	0.109571	0.0097
640	0.108645	0.0087
832	0.108478	0.0086
1024	0.108396	0.0085
1760	0.108225	0.0083
2048	0.108168	0.0082

and  $L$  ranging from 4 to 100. Fig. 4 presents the *average distortion gap to the RD limit*  $\bar{\delta} \triangleq \bar{D} - D_{Sh}$  obtained with respect to codeword length for SC(3, 6), SC(4, 8), and SC(5, 10) codes. It can be seen from Fig. 4 that the average distortion gap decreases roughly exponentially with  $L$  and saturates to a value close to the RD limit; moreover, for fixed  $M$ , the gap decreases with increasing density  $J$ .<sup>2</sup>

3) *Effect of Increasing the Lifting Factor  $M$* : Table I shows the effect of increasing  $M$ . Here we consider SC(4, 8) codes with fixed  $L = 16$ ,  $R_L = 0.5313$ , and RD limit  $D_{Sh} = 0.09992$ . We observe that, as expected, increasing  $M$  reduces the average distortion and we obtain saturating values that approach the RD limit. Since SC-LDGM codes experience saturation in their distortion values both for increasing  $L$  and  $M$ , combining these results (by letting  $M \rightarrow \infty$  and  $L \rightarrow \infty$ ) implies that SC( $J, K$ ) codes numerically approach the optimal distortion values of the underlying ( $J, K$ )-regular LDGM-BCs. For example, for a relatively large SC(4, 8) code with  $L = 100$ ,  $M = 512$ , and  $R_L = 0.5050$ , we obtained an average distortion of  $\bar{D} = 0.113463$ , where the optimal average distortion of a (4, 8)-regular LDGM-BC of  $R_L = 0.5$  is  $\bar{D}_{opt} = 0.1111$  [27].

<sup>2</sup>Note that the compression rate varies according to (2). Each point was compared to the RD limit for the given rate.

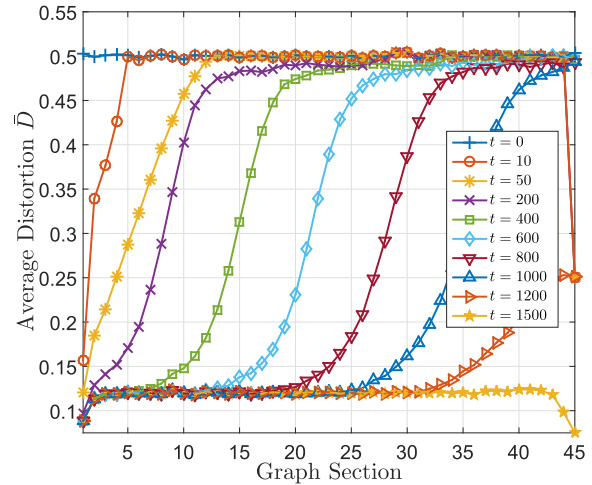


Fig. 5. Average distortion evolution of an SC(3, 6) code with  $L = 45$  and  $M = 512$  for various numbers of iterations of Algorithm A.

4) *Wave-Like Encoding*: Fig. 5 shows the average distortion evolution over each section of the graph of an SC(3, 6) code with  $L = 45$ ,  $M = 512$ , and a total of 23,552 code nodes for various numbers of iterations  $t$  of Algorithm A. Note that the behavior is similar to the wave-like decoding of SC-LDPC codes for channel coding [32], where the code nodes at the left end of the graph generate large bias values (reliable information, thereby starting the decimation process), which then propagate through the graph from left to right with increasing iterations. Initially, the average distortion is around 0.5, but after a few iterations the degree two generator nodes (at the left side of the graph) facilitate convergence of the attached code nodes, thereby generating large bias values and starting an “encoding wave” (see also the following subsection). Note that if we decimate a single code node per iteration, the algorithm requires 23,552 iterations to terminate, but Fig. 5 shows that after decimating only 1500 code nodes, the bias values have already saturated and the algorithm can be stopped.

The wave-like encoding phenomenon and propagation of reliable bias values from left to right motivates the use of a windowed encoding scheme, where we modify the decimation progress during the encoding wave, thereby reducing both computational complexity and encoding latency. For example, the complexity can be reduced by decimating multiple code nodes per iteration. This could be done in a fixed way, *i.e.*, by decimating  $x$  nodes per iteration, or by using threshold values, *i.e.*, by decimating nodes only when a sufficiently large bias value is obtained. Both approaches are discussed in Section IV.

5) *Effect of the Generator Node Degrees at the Ends of the Code Graph*: As mentioned in Section II, we choose to modify the SC-LDGM protograph in (1) to reduce the generator node degrees at the left end of the graph to facilitate propagation of reliable information via wave-like encoding. In this section, we demonstrate how the choice of the generator node degrees affects the initialization and propagation of the encoding wave. As an example, we construct a (4, 8)-regular SC-LDGM base matrix in the form of (1) with  $\mathbf{B}_0 = \mathbf{B}_1 = \mathbf{B}_2 = \mathbf{B}_3 = [1, 1]$

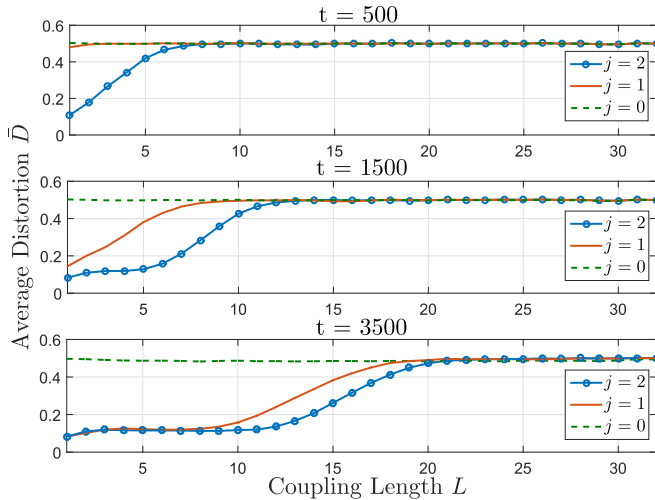


Fig. 6. Average distortion distribution among coupled sections of SC(4, 8) codes with  $L = 32$ ,  $M = 512$ , and the first  $j$  rows deleted.

and consider deleting the first  $j = 0, 1$ , and 2 rows. For  $j = 0$ , all generator nodes (columns of (1)) in the graph have degree 4, while the code nodes (rows of (1)) have degrees 2, 4, 6, 8, 8,  $\dots$ ; for  $j = 1$ , the generator nodes in Section 1 (column 1 of (1)) have a reduced degree of 3 and the code node degrees are 4, 6, 8, 8,  $\dots$ ; finally, for  $j = 2$ , the generator nodes in Sections 1 and 2 (columns 1 and 2 of (1)) have degrees 2 and 3, respectively, while the code nodes have degrees 6, 8, 8,  $\dots$ .

Fig. 6 shows snapshots of the encoding process with soft-hard decimation at  $t = 500, 1500$ , and 3500 iterations (from top to bottom) for the 3 constructions obtained with  $j = 0, 1$ , and 2 rows deleted and with code parameters  $L = 32$  and  $M = 512$ . We observe that, by iteration  $t = 500$ , the average distortion of the leftmost sections of the  $j = 2$  construction has decreased faster than the other constructions and the wave-like behavior has begun. On the other hand, the  $j = 1$  construction shows only a slight improvement, while the  $j = 0$  construction has not shown any improvement and has average distortion  $\bar{D} = 0.5$  over all sections. By iteration  $t = 1500$ , the encoding of Section 5 of the  $j = 2$  construction is almost complete (the code nodes in this section have almost reached their final values) and the wave has reached Section 12; meanwhile, for  $j = 1$ , we observe the distortion has now improved at the leftmost end and the wave-like behavior is visible; however, we still see no improvement for  $j = 0$ . Finally, by iteration  $t = 3500$ , we observe that the encoding wave for  $j = 1$  and  $j = 2$  are now steadily moving through the chain, with the  $j = 2$  construction reaching further due to its earlier advantage; however, there is still no significant distortion improvement for  $j = 0$ .

The reduced generator nodes not only increase convergence/wave propagation speed, they also have an impact on the resulting distortion. Fig. 7 shows the average distortion results per graph section obtained for the  $j = 0, 1$ , and 2 constructions after encoding is completed. The poor performance of the  $j = 0$  construction with soft-hard decimation can be explained by investigating the encoding progress across the

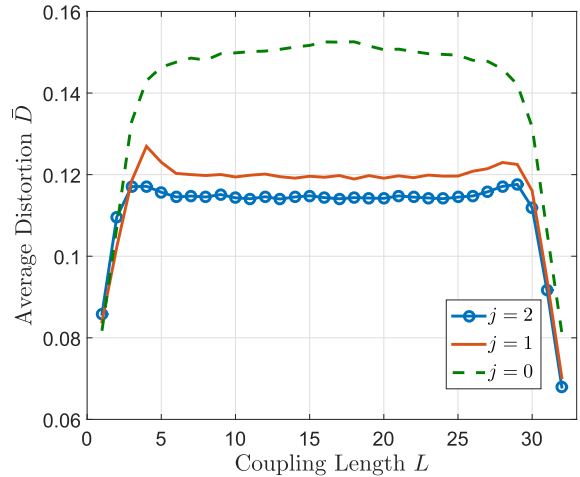


Fig. 7. Average distortion performance of SC(4, 8) codes with  $L = 32$ ,  $M = 512$ , and the first  $j$  rows deleted.

graph sections at different iterations  $t$ . We saw in Fig. 6 that the distortion decreases slowly at the right end of the graph; however, Algorithm A still enforces decimation at each iteration. We observed experimentally that roughly the first one-sixth of decimated code nodes occurred randomly throughout the graph with low reliability (bias values near 0). Eventually, though, the distortion decreases at the ends and the wave-like encoding begins; however, those initial decimated code nodes with low reliability result in a high overall distortion, as seen in Fig. 7. For  $j = 1$ , by around iteration  $t = 1000$ , the code nodes decimated by Algorithm A at the left end of the graph have reasonably good reliability (bias values about 0.7) and low distortion values; after that, the encoding wave proceeds, decimating code nodes with high reliability (bias values about 0.9). Note that the initial improvement in convergence compared to the  $j = 0$  case significantly lowers the overall distortion as the encoding wave travels through the graph. For  $j = 2$ , the algorithm quickly converges, with distortion decreasing rapidly over the leftmost sections of the graph as code nodes are decimated with high reliability (bias values about 0.9) by around iteration  $t = 40$ . This generates an encoding wave that propagates through the graph from left to right. Thus the  $j = 2$  construction outperforms the others with Algorithm A as a result of better “seeding” of the wave, with more reliable information generated at the ends of the graph. Moreover, as the wave reaches the right end of the (non-symmetric) graph, all nodes are decimated with high reliability and the distortion is low.

Although our primary interest is to take advantage of the convolutional structure of the code and track the propagation of the encoding wave from left to right with a sliding window (see Section IV), where the right end of the graph is not involved until the end of the encoding process, it is also interesting to investigate the effect of modifying the right end of the chain when using Algorithm A. Suppose we remove the first  $j_1$  rows and the last  $j_2$  rows of (1). In the previous  $j = 2$  case, now denoted  $\mathbf{j} = (j_1 = 2, j_2 = 0)$ , the degree 4 generator nodes at the right do not create a wave (as we

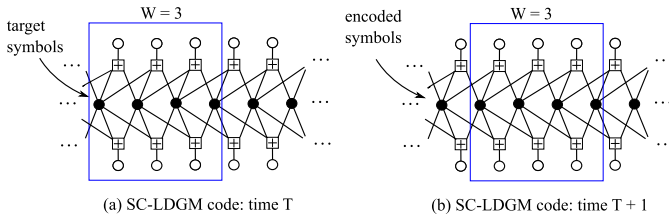


Fig. 8. The WE procedure operating on the protograph of an SC(3, 6) code.

saw in the  $j = 0$  case above) and a single encoding wave propagates from left to right, but this is not the case if we also reduce the generator degrees at the right, *i.e.*, we choose  $j_2 > 0$ . For example, consider  $\mathbf{j} = (2, 2)$ ,  $(2, 1)$ , and  $(1, 1)$ , for the  $(4, 8)$ -regular construction. In the  $\mathbf{j} = (2, 2)$  and  $\mathbf{j} = (1, 1)$  cases, encoding waves propagate from both sides of the graph (much like they do in the  $j = 2$  and  $j = 1$  cases above), but, interestingly, when the waves meet in the center there is disagreement and the average distortion increases, since this disagreement ripples out from the center back to the ends via undecimated nodes. In general, we find that symmetric codes result in higher distortion for the reasons discussed above. In the  $\mathbf{j} = (2, 1)$  case, the encoding waves start independently from both ends of the graph, but the left wave moves faster, resulting in higher distortion at the right side of the code graph. As an interesting aside, we note that this behavior is not observed in the case of BP decoding of SC-LDPC codes, where there are not multiple optimal solutions and the decoding waves are typically in agreement.

#### IV. WINDOWED ENCODING

For the practical implementations of SC-LDGM codes with large coupling length  $L$ , it is essential to reduce the encoding latency. To this end, we propose a novel sliding window encoder, where a window of size  $W$  (containing  $W$  sections of the graph) slides over the graph from left to right. This is a similar concept to the sliding window decoder for channel coding with SC-LDPC codes [33]. At each window position, a modified BP algorithm (*e.g.*, Algorithm A) is applied to the code nodes in the window and all their neighboring generator nodes in order to encode one set of code symbols, called *target symbols*. After encoding the set of target symbols (*i.e.*, when they are all decimated), the window slides one section to the right and again executes the modified BP algorithm to encode the next set of target symbols, using both the nodes in the window and some previously encoded target symbols. Fig. 8 shows the WE procedure on the protograph of a SC(3, 6) code with window size  $W = 3$  (covering 3 graph sections, or  $3M$  code symbols). Here  $2M$  source symbols enter the window at each window position and  $M$  code symbols leave (are encoded). In this paper, we refer to the *latency* of a WE scheme as the number of source symbols in the window, *i.e.*, how many source symbols we need to process before we can encode a set of target symbols. Full details of WE with two modifications for efficiency, termed Algorithms B and C, follow in the next two sections.

##### A. Multiple Node Decimations Per Iteration (Algorithm B)

To reduce the number of required iterations, thereby reducing complexity, we consider modifying the algorithm to

decimate the  $N \geq 1$  code nodes with the highest bias values. In order to generate reliable messages and low distortion at the left end of the graph (initial nodes), (4), (5), and (6) are applied for a fixed number of iterations,  $I_f$ , to build reliable bias values before decimation begins. Details of this process are given in Algorithm B. In addition to the previous notation,  $W^{(t)}$  denotes the window at iteration  $t$ ,  $W_Z^{(t)}$  denotes the set of code nodes inside the window,  $W_G^{(t)}$  denotes the set of generator nodes inside the window, and  $T(W^{(t)})$  denotes the set of target symbols inside the window. Finally, we use  $W_{Z_p}^{(t)}$  and  $W_{Z_f}^{(t)}$  to denote the set of past code nodes (to the left of the window) and future code nodes (to the right of the window), respectively, and  $W_{G_p}^{(t)}$  and  $W_{G_f}^{(t)}$  are defined similarly. The initial code to generator node messages,  $R_{i \rightarrow a}^{(0)}$ , are set to  $\pm 0.1$ , with  $\mathbb{P}(R_{i \rightarrow a}^{(0)} = 0.1) = 0.5$  and reset to 0 at iteration 1.

---

#### Algorithm B Multiple Node Decimation

---

- 1) At iteration  $t = 0$ , initialize the graph to  $\Gamma^{(t=0)}$
  - 2)  $\forall i \in W_Z^{(t)}, a \in W_G^{(t)}$  update (4), (5), and (6) for  $I_f - 1$  iterations such that
    - a) there is no incoming or outgoing message  $\forall a \in W_{G_f}^{(t)}$
    - b) there are incoming messages  $\forall i \in W_{Z_p}^{(t)}$  and  $\forall a \in W_{G_p}^{(t)}$ , but no outgoing messages to those nodes
  - 3)  $\forall i \in W_Z^{(t)}, a \in W_G^{(t)}$  update (4), (5), and (6) according to 2a) and 2b)
  - 4) Find the  $N$  largest bias values among the remaining target symbols  $B^{(t)} = \{B_i^{(t)} \mid i \text{ not fixed}, i \in T(W^{(t)})\}$
  - 5) For each of the  $N$  selected biases  $i$ , do:
    - a) **if**  $B_i^{(t)} > 0$  then  
 $z_i \leftarrow '1'$   
**else**  
 $z_i \leftarrow '0'$   
**end if**
    - b) decimate graph as
      - i)  $\forall a \in G(i), s_a \leftarrow s_a \oplus z_i$  (update source symbols)
      - ii) reduce the graph as  $\Gamma^{(t+1)} = \Gamma^{(t)} \setminus \{i\}$  (remove code node  $i$  and all its edges)
  - 6) **if** there exist any unassigned code symbols  $i \in T(W^{(t)})$ , go to 3)  
**else if** all source symbols are not encoded, shift window to the next position, go to 3)  
**else** exit algorithm  
**end if**
- 

1) *Windowed Encoding Results for  $N = 1$* : In this section, we present numerical results for WE of SC(4, 8) codes with  $N = 1$  and  $I_f = 0$  as an example. (Similar results were also obtained for other values of  $J$  and  $K$ .) Note that, by setting  $N = 1$ , Algorithm B can be thought of as the application of Algorithm A within a window. Also, like Algorithm A, the performance of the WE algorithm is sensitive to the

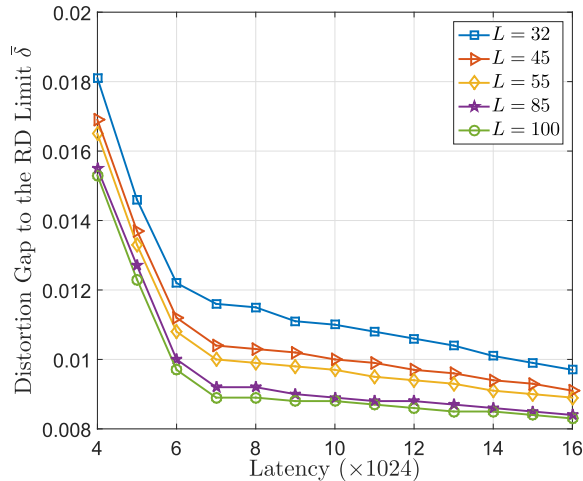


Fig. 9. Average distortion gap to the RD limit for various SC(4,8) codes with increasing latency (window size  $W$ ).

choice of  $\xi$ , which was determined numerically for each code ensemble.

We considered an SC(4,8) code with  $L = 100$ ,  $M = 512$ , rate  $R_L = 0.5050$ , and RD limit  $D_{Sh} = 0.1084$ . Applying Algorithm B (windowed encoding with  $N = 1$ ) with  $W = 10$  and  $\xi = 0.02$ , the average distortion is  $\bar{D} = 0.1172$ , while applying Algorithm A (block encoding) gives  $\bar{D} = 0.1135$ , indicating there is only a slight loss in performance for a sufficiently large  $W$ . Fig. 9 shows the average distortion gap to the RD limit  $\bar{\delta}$  (adjusted for the compression rate) for several SC(4,8) LDGM code lengths  $L$  and window sizes  $W = 4, 5, \dots, 16$ , with fixed  $M = 512$ , where the encoding latency is equal to  $2MW$ . We observe that by increasing the code length and latency, the average distortion saturates to a value close to the RD limit for the given rate. We also see that increasing  $W$  (latency) beyond a certain value improves the distortion only slightly. For example, we note that only moderate improvements in distortion are obtained by increasing  $W$  beyond 8.

Fig. 10 plots the average distortion as a function of latency obtained by applying Algorithm B (with  $N = 1$ ) to SC(4,8) codes with  $L = 32$ , compression rate  $R = 0.5156$ , and  $W = 4, 5, \dots, 12$  for  $M = 512, 1024$ , and 2048, respectively. Also plotted for comparison is the average distortion of an irregular LDGM-BC (optimized for the soft decimation algorithm) with compression rate  $R = 0.5$  and degree distribution [25]

$$\lambda(x) = x^6, \quad (8)$$

$$\rho(x) = 0.275698x + 0.25537x^2 + 0.076598x^3 + 0.39233x^8. \quad (9)$$

Note that the latency of the LDGM-BC is its total block length, and each point on the LDGM-BC curve corresponds to a code drawn from the irregular ensemble with a particular latency. We observe that the *regular* SC-LDGM codes outperform the irregular LDGM-BC as long as  $W$  is not too small and that performance tradeoffs can be achieved for SC-LDGM codes by varying  $M$  and  $W$ . In particular, increasing  $W$  improves

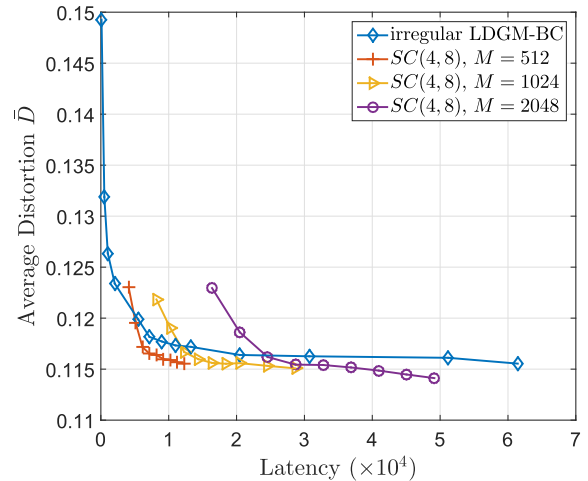


Fig. 10. Average distortion versus latency of (4,8)-regular SC-LDGM codes with different lifting factors and  $L = 32$  compared to optimized, irregular LDGM-BCs. Latency for the SC-LDGM code corresponds to the window size, whereas the latencies for the LDGM-BCs correspond to their block lengths.

the performance of the encoder, while increasing  $M$  improves the performance of the code.

2) *Windowed Encoding Results for  $N > 1$* : Instead of decimating one code node at each iteration, we now set Algorithm B to decimate the  $N > 1$  code nodes with the largest bias values. All numerical results presented are obtained by averaging over 1000 trials using an SC-LDGM code SC(4,8) with coupling length  $L = 55$ , lifting factor  $M = 512$ , and window size  $W = 8$ , so the latency  $2MW = 8192$  symbols and the compression rate  $R_L = 0.5091$ . For reference, the average distortion using Algorithm A (block encoding) is  $\bar{D}_A = 0.112767$  after performing 28,672 iterations.

We measure the *complexity* of the algorithm as the average number of updates  $\bar{I}$  that a code node receives, averaged over the entire graph. Since these codes will typically operate in a regime with moderate to large  $L$ , we also present the average number of updates per node for nodes *outside* the initial window position, referred to as the average “*steady-state*” number of updates  $\bar{I}_{ss}$ , which is constant and larger than  $\bar{I}$ , since the nodes in the initial window position typically (depending on  $I_f$ ) require fewer updates. We note that both  $\bar{I}$  and  $\bar{I}_{ss}$  depend on  $W$ , but, while  $\bar{I}_{ss}$  is independent of  $L$ ,  $\bar{I}$  depends (slightly) on  $L$ . Consequently, we use  $\bar{I}_{ss}$  to compare with Algorithm A, for which the average number of updates per code node is given by  $\bar{I}_A = \frac{m(m+1)}{2m} = \frac{m+1}{2}$ , where  $m$  is the number of code nodes. In this example,  $\bar{I}_A = 14,337$ .

Table II shows the performance of Algorithm B compared to Algorithm A, in terms of the *average distortion loss* (measured as  $\frac{\bar{D} - \bar{D}_A}{\bar{D}_A}$ ) and the *average complexity savings* (measured as  $\frac{\bar{I}_A - \bar{I}_{ss}}{\bar{I}_A}$ ), both given as percentage values, for the SC(4,8) example with  $I_f = 10$  and various values of  $N$ . We note that by increasing the number  $N$  of decimated code nodes at each iteration the complexity decreases accordingly; however, the distortion increases. For example, by decimating

TABLE II  
AVERAGE DISTORTION AND COMPLEXITY RESULTS FOR  
ALGORITHM B COMPARED TO ALGORITHM A

$N$	$\bar{D}$	Distortion Loss (%)	$\bar{I}$	$\bar{I}_{ss}$	Complexity savings (%)
1	0.116905	3.6704	3975.80	4352.40	69.6422
2	0.117226	3.9542	1991.80	2176.50	84.8185
3	0.117680	4.3568	1332.30	1453.80	89.8594
4	0.118159	4.7815	999.75	1088.50	92.4075
8	0.119842	6.2740	503.75	544.50	96.2020
10	0.120622	6.9657	409.81	442.11	96.9162
20	0.122804	8.9007	208.51	221.28	98.4565
40	0.125296	11.1105	107.86	110.89	99.2265

$N = 2$  code nodes per iteration, the algorithm complexity reduces to 84.82% at a cost of only 3.95% in distortion, whereas decimating  $N = 10$  nodes per iteration results in a complexity reduction of 96.92% at a cost of 6.97% in distortion. By further increasing  $N$  to 20 (resp. 40) we obtain an average complexity savings of 98.46% (resp. 99.23%), but this costs 8.90% (resp. 11.11%) in distortion. We also note that, for  $I_f = 10$ , the savings in total complexity  $\bar{I}$  is even larger, and that the complexity savings grows with increasing  $L$ . We will see in the next subsection that such reductions in complexity can be achieved with much smaller losses in distortion by implementing a thresholding scheme.

### B. Thresholding (Algorithm C)

Instead of decimating a fixed number of nodes per iteration, the thresholding algorithm decimates all code nodes that have bias values greater than a pre-selected threshold  $\theta$  after  $I_h$  iterations. The details are given in Algorithm C. Similar to Algorithm B, it is necessary to update the nodes in the first window position a sufficient number of times ( $I_f$  iterations) in order to generate bias values large enough to propagate through the chain. To insure termination, if no unassigned target node achieves a bias value larger than  $\theta$  for 10 consecutive iterations, all remaining target nodes are decimated and the window shifts to the next position. Also, the parameter  $I_h$ , which can be used to control the speed of decimation, is normally set to 1, *i.e.*, we decimate after each iteration.<sup>3</sup> (Unless otherwise noted, we set  $I_h = 1$  in the remainder of the paper.)

1) *Numerical Results and Encoder Dynamics of Thresholding:* Table III shows the performance of Algorithm C compared to Algorithm A for various threshold values  $\theta$  and  $I_f = 100$ . We observe that the thresholding scheme provides a significant complexity savings compared to the benchmark case (more than 98% for all threshold values). Also, as expected, we observe that large threshold values  $\theta$  provide good average distortion  $\bar{D}$  but require more iterations (large  $\bar{I}_{ss}$ ), whereas decreasing  $\theta$  results in fewer iterations at a cost of larger distortion. We further note that decimation with thresholding can achieve similar reductions

<sup>3</sup>In certain cases, *e.g.*, for large windows or high degree codes, thresholding can generate large bias values quickly, which can cause the algorithm to decimate too fast. In this case, complexity is low but the distortion can be unacceptably large. This can be controlled by increasing  $I_h$ .

### Algorithm C Threshold Decimation

- 1) At iteration  $t = 0$ , initialize the graph to  $\Gamma^{(t=0)}$  and set a *counter*  $\leftarrow 10$
- 2)  $\forall i \in W_Z^{(t)}, a \in W_G^{(t)}$  update (4), (5), and (6) for  $I_f - 1$  iterations such that
  - a) there is no incoming or outgoing message  $\forall a \in W_{G_f}^{(t)}$
  - b) there are incoming messages  $\forall i \in W_{Z_p}^{(t)}$  and  $\forall a \in W_{G_p}^{(t)}$ , but no outgoing messages to those nodes
- 3)  $\forall i \in W_Z^{(t)}, a \in W_G^{(t)}$  update (4), (5), and (6) for  $I_h$  iterations, under the same conditions as 2)
- 4) For each remaining bias value  $B_i^{(t)}$ ,  $i$  not fixed,  $i \in T(W^{(t)})$ , do
  - IF**  $|B_i^{(t)}| \geq \theta$  then
    - a) **if**  $B_i^{(t)} > 0$  then
      - $z_i \leftarrow '1'$
      - else**
      - $z_i \leftarrow '0'$
      - end if**
    - b) decimate graph as
      - i)  $\forall a \in G(i)$ ,  $s_a \leftarrow s_a \oplus z_i$  (update source symbols)
      - ii) reduce the graph as  $\Gamma^{(t+1)} = \Gamma^{(t)} \setminus \{i\}$  (remove code node  $i$  and all its edges)
    - c) *counter*  $\leftarrow 10$
    - end if**
  - 5) **IF** no nodes were decimated in Step 4) then
    - counter*  $\leftarrow$  *counter*  $- 1$
    - IF** *counter* = 0
      - For  $\{B_i^{(t)} \mid \forall i \text{ not fixed}, i \in T(W^{(t)})\}$ , decimate  $B_i^{(t)}$  according to 4a) and 4b)
      - counter*  $\leftarrow 10$
      - else** go to 3)
      - end if**
    - end if**
  - 6) **if** there exist any unassigned code symbols  $i \in T(W^{(t)})$ , go to 3)
    - else if** all source symbols are not yet encoded, shift window to the next position, go to 3)
    - else** exit algorithm
    - end if**

in complexity as decimating the best  $N$  nodes, but with better distortion. For example, both  $N = 40$  (Algorithm B) and  $\theta = 0.90$  (Algorithm C) have  $\bar{I}_{ss} \approx 110$ , but with average distortion losses of 11.11% and 6.19%, respectively. The improvement is also significant when comparing  $N = 20$ , with  $\bar{I}_{ss} \approx 220$ , to  $\theta = 0.9999$ , with  $\bar{I}_{ss} \approx 200$ , resulting in distortion losses of 8.90% and 4.19%, respectively. Moreover, it is simpler to compare each remaining target bias value to a threshold  $\theta$  (Alg. C) than to find the  $N$  largest bias values (Alg. B); however, Alg. B provides a fixed complexity and run-time, whereas the complexity of Alg. C can vary.

TABLE III  
AVERAGE DISTORTION AND COMPLEXITY RESULTS FOR  
ALGORITHM C COMPARED TO ALGORITHM A

Threshold value $\theta$	$\bar{D}$	Distortion Loss (%)	$\bar{I}_{ss}$	Complexity savings (%)
0.9999	0.117495	4.1927	202.37	98.5884
0.999	0.117977	4.6201	167.21	98.8337
0.99	0.118411	5.0050	137.04	99.0441
0.90	0.119747	6.1898	112.40	99.2160
0.80	0.120408	6.7759	105.71	99.2627

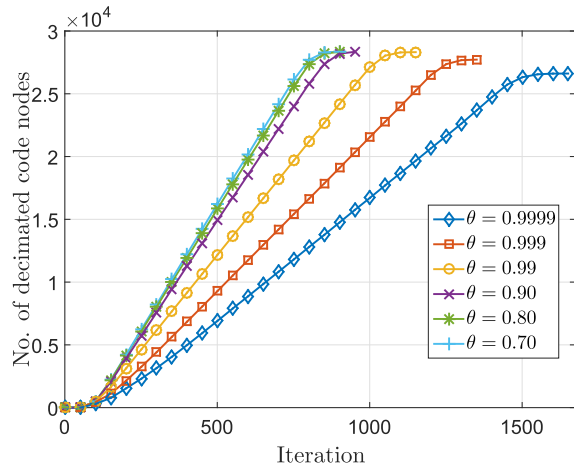


Fig. 11. Cumulative number of decimated code nodes at each iteration for different threshold values  $\theta$ .

Fig. 11 shows the cumulative number of decimated code nodes at each iteration for various  $\theta$ . We observe that the algorithm has three phases:

- 1) the *initialization phase*, where we perform  $I_f$  iterations without hard decimation;
- 2) the *steady-state phase*, where the window moves at a constant speed over the graph (seen as an approximate straight line with slope  $\Delta$  in Fig. 11); and
- 3) the *termination phase*, where the window reaches the end of the graph and the number of decimated nodes per iteration decreases to zero.

In particular, we see that the slope  $\Delta$  in the steady-state phase indicates that the algorithm decimates approximately  $\Delta$  code nodes per iteration as the window moves over the graph and that  $\Delta$  is larger for lower thresholds  $\theta$ . The values of  $\Delta$  are shown in Table IV, where we note that the decimation rate roughly doubles from  $\theta = 0.9999$  to  $\theta = 0.70$  and, assuming that a large  $L$  will be used in practice, the performance is dominated by the steady-state phase. Also given in Table IV are the values obtained for the *average steady-state distortion*  $\bar{D}_{ss}$ , obtained as the average distortion over all nodes excluding those at the ends (initialization and termination phases), along with the average number of steady-state node updates  $\bar{I}_{ss}$ . The results indicate that  $\bar{D}_{ss}$  approaches the overall average distortion  $\bar{D}$  for large  $\theta$ , with relatively low complexity, which in turn approaches the RD limit for (4,8)-regular LDGM codes [27] with increasing  $M$ . We also see that relaxing the threshold results in higher steady-state distortion but lower complexity.

TABLE IV  
PERFORMANCE OF ALGORITHM C IN THE STEADY-STATE PHASE

Threshold value $\theta$	$\Delta$	$\bar{D}_{ss}$	$\bar{I}_{ss}$
0.9999	20.3918	0.1181	202.3663
0.999	24.6209	0.1184	167.2043
0.99	30.1674	0.1191	137.0379
0.90	36.7937	0.1204	112.3921
0.80	39.2504	0.1214	105.7014
0.70	40.1335	0.1216	103.1221

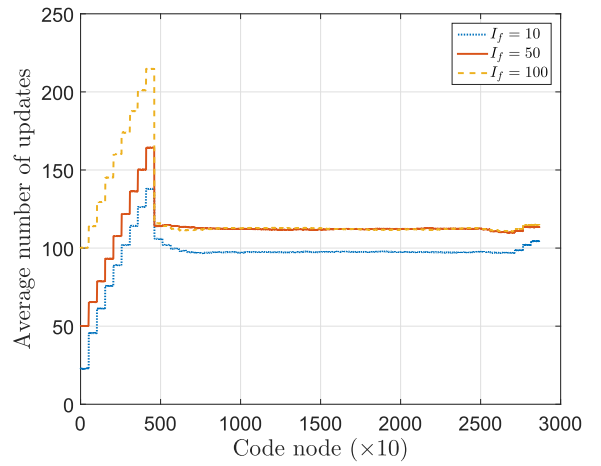


Fig. 12. Average number of updates per code node for various  $I_f$ .

Due to the initialization phase, the complexity is also affected by  $I_f$ . Fig. 12 shows the complexity, measured as the average number of updates per code node, as a function of position in the graph, for  $\theta = 0.90$  and  $I_f = 10, 50,$  and  $100$ . Again, we observe that the encoding can be divided into three phases: initial, steady-state, and termination. Since  $W = 8$  and  $M = 512$ , the first 9 sections ( $9M = 4608$  code nodes) automatically receive at least  $I_f$  updates (cf. Fig. 2). This is evident as the “steps” in Fig. 12. As the algorithm progresses, we reach the steady-state phase where the complexity and the decimation rate  $\Delta$  are constant (see also Fig. 11). We note that the number of updates in the latter positions of the initial window exceeds the steady-state values, due to the offset of  $I_f$ , but that this behavior is less pronounced for small values of  $I_f$ . Finally, we reach the termination phase, where Fig. 12 shows a slight increase in complexity. Table V summarizes the distortion results for  $\theta = 0.90$  and various values of  $I_f$ . We observe that, by increasing  $I_f$ , the distortion decreases and the complexity increases, and we note that it is important to have a sufficiently large  $I_f$  to generate reliable bias values, but increasing  $I_f$  further offers diminishing gains.

2) *SC-LDGM Thresholding Performance for Different Compression Rates*: Although we have focused on SC-LDGM code ensembles with nominal compression rate  $R = 0.5$ , similar performance can be observed for a variety of compression rates, with and without WE. Fig. 13 summarizes simulation results of the average steady-state distortion  $\bar{D}_{ss}$  for various compression rates  $R$  compared to the corresponding RD limit.  $(J, K)$ -regular SC-LDGM codes with

TABLE V  
AVERAGE DISTORTION RESULTS FOR  $\theta = 0.90$  AND VARIOUS  $I_f$

$I_f$	$\bar{D}$	$\bar{D}_{ss}$	$\bar{I}_{ss}$
500	0.1197	0.1204	112.6404
100	0.1197	0.1204	112.3921
50	0.1202	0.1205	112.1783
10	0.1232	0.1236	97.4348

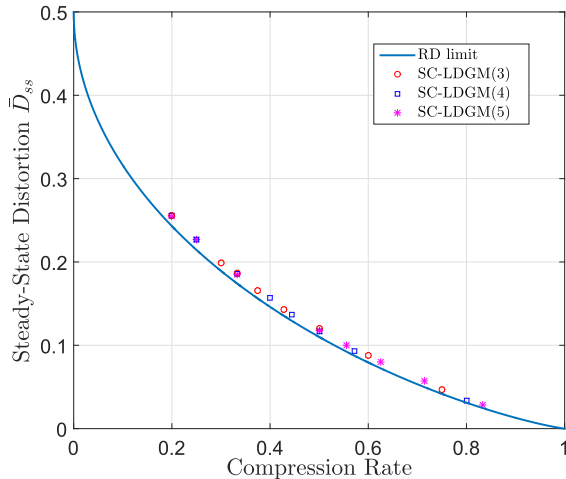


Fig. 13. Average steady-state distortion of SC-LDGM codes for three different generator node degrees  $J$  and various compression rates.

fixed generator node degree  $J$  were constructed, which we denote by LDGM( $J$ ). The constructed codes have lifting factor  $M = 512$ , which results in an overall LDGM code length of approximately 100,000. They were encoded using Algorithm C, with  $\theta = 0.9999$ , window size  $W = 7$ ,  $\xi$  optimized to three decimal places,  $I_f = 100$ , and  $I_h = 14$  iterations between two successive decimation steps.<sup>4</sup>

As can be seen from Fig. 13, the distortion is very close to the RD limit in all cases. We also observe that by increasing the rate, the average distortion gap to the RD limit is diminishing. Furthermore, we note that the distortion of the LDGM( $J$ ) ensembles approaches the RD limit as the generator node degree  $J$  increases. These results were not optimized on a case-by-case basis (with the exception of  $\xi^*$ ); indeed, the simulation parameters were simply chosen such that we expected “good” performance. Consequently, they can likely be improved in terms of providing a better latency/complexity trade-off for a given distortion by optimizing parameters, such as the protograph structure, further increasing the accuracy of  $\xi^*$ , and adjusting the threshold  $\theta$ , the number of initial iterations  $I_f$ , the number of iterations between decimation steps  $I_h$ , and the window size  $W$ .

#### C. A Complexity and Latency Comparison With LDGM-BCs

This section briefly compares the proposed protograph-based SC-LDGM codes with an example of a state-of-the-art, highly irregular LDGM-BC that was optimized for the

<sup>4</sup> $I_h = 14$  was chosen here since it results in good distortion for all cases considered in Fig. 13. This value can be reduced to  $I_h = 1$  in many cases without significant loss in distortion, as seen earlier for some  $(J, 2J)$ -regular ensembles.

TABLE VI  
SOFT DECIMATION [25] RESULTS FOR AN IRREGULAR LDGM-BC WITH  $n = 8192$  AND RATE  $R_L = 0.5$  (RD LIMIT 0.11)

Algorithm iterations	$\bar{D}$
202	0.119420
167	0.120095
137	0.120855
112	0.121955
105	0.122237
103	0.122309

soft-decimation algorithm [25]. We showed in Section IV-A that, on an equal latency basis, the *regular* SC(4, 8) SC-LDGM code encoded with WE outperformed an optimized *irregular* code. For the purpose of illustration, we now fix the latency to be 8192 symbols and allow the complexity to vary for comparison. The irregular LDGM-BC is constructed with degree distribution as given in (8) and (9) following [25] and the SC(4, 8) code is constructed with  $M = 512$  and encoded with  $W = 8$ . Comparing Tables IV (for the SC-LDGM code) and VI (for the LDGM-BC), we see that, for equal rate and fixed latency, the average steady-state distortion  $\bar{D}_{ss}$  of the regular SC-LDGM code is less than the average distortion  $\bar{D}$  of the optimized irregular LDGM-BC when the average number of steady-state node updates  $\bar{I}_{ss}$  of the SC-LDGM code equals the number of iterations of the LDGM-BC. Further gains for the SC-LDGM code may be possible by optimizing the code construction and the windowed encoder parameters.

#### D. Min-Sum Algorithm

Following well-established procedures from the channel coding literature to achieve good performance-complexity trade-offs, the proposed decimation algorithm can be simplified by approximating the generator node to code node message using a simple minimum operation, known as the min-sum algorithm. For this purpose, (5) is replaced with

$$R_{a \rightarrow i}^{(t+1)} = \frac{1}{\mu} R_{i \rightarrow a}^{(t)} + \gamma (-1)^{s_a + |Z(a)|} \left( \prod_{j \in Z(a) \setminus i} \alpha_{j \rightarrow a}^{(t)} \right) \min\{\psi\}; \quad (10)$$

where  $\gamma < 1$  is a constant scaling factor,  $\alpha_{j \rightarrow a}^{(t)} = \text{sign}(R_{j \rightarrow a}^{(t)})$ , and  $\psi = \{|R_{j \rightarrow a}^{(t)}|\}_{j \in Z(a) \setminus i}$  (see [34] for more details.)

To obtain results for the min-sum algorithm, we limited the magnitudes of all messages (code to generator node and generator to code node) to 20 and used  $\gamma = 0.5$ .<sup>5</sup> Then, replacing (5) with (10) in Alg. A (block encoding) for an SC(4, 8) code with coupling length  $L = 55$  and lifting factor  $M = 512$ , we obtained distortion  $\bar{D} = 0.114440$  (compared to the BP version of Alg. A with  $\bar{D}_A = 0.112767$ ). In addition, we investigated the effect of the lifting factor  $M$  using the min-sum algorithm for some of the codes given in Table I.

<sup>5</sup>Several approaches could be taken here to improve distortion performance, such as optimizing the pair  $(\xi, \gamma)$ , allowing  $\gamma$  to vary over iterations, or applying a normalized version of the min-sum algorithm.

TABLE VII

EFFECT OF THE LIFTING FACTOR  $M$  FOR THE MIN-SUM ALGORITHM ON SC(4, 8) CODES IN TERMS OF AVERAGE DISTORTION  $\bar{D}$  AND AVERAGE GAP TO THE RD LIMIT  $\bar{\delta}$  WITH FIXED  $L = 16$  AND COMPRESSION RATE  $R_L = 0.5313$

Lifting factor ( $M$ )	$\bar{D}$	$\bar{\delta}$	Deviation from BP Alg. (%)
256	0.111921	0.0120	1.6780
640	0.110373	0.0105	1.5905
832	0.110035	0.0101	1.4353
1024	0.109860	0.0100	1.3506
2048	0.109314	0.0094	1.0595

The obtained distortions are shown in the Table VII, where we see that the performance degradation is very slight (less than 1.68%) and decreases with increasing lifting factor  $M$  for the min-sum case.

## V. CONCLUSION

In this paper, we introduced a new construction of  $(J, K)$  regular SC-LDGM codes based on protographs for lossy source coding. The proposed “soft-hard” BP-based decimation algorithm was shown to perform well, giving average distortion values close to the RD limit. We then presented a novel low-latency WE algorithm with two decimation approaches that can significantly lower complexity (measured as the number of node updates) with little performance degradation for a sufficiently large window size, allowing good source reconstruction performance to be obtained for moderate encoding latency. The first technique decimates a fixed number of nodes per iteration and the second decimates all nodes with sufficiently large confidence at each iteration. We showed that a significant reduction in complexity ( $> 90\%$ ) can be achieved compared to decimating a single node per iteration, with only moderate losses in distortion. Also, we showed that a min-sum formulation can be used during the BP updates that further reduces the complexity at the cost of a slight loss in performance. There are several features of WE approach that can be improved, such as designing good convolutional protographs that permit shorter window sizes and optimizing message passing schedules within an encoding window. This, along with a study of the performance for more general sources, is the subject of ongoing work.

## ACKNOWLEDGEMENTS

The authors would like to thank the reviewers for their constructive comments to improve the presentation of the paper. In particular, the comments of Reviewer 1 regarding the introduction of a min-sum formulation are especially appreciated.

## REFERENCES

- [1] T. Goblick, “Coding for a discrete information source with a distortion measure,” Ph.D. dissertation, Massachusetts Inst. Technol., Cambridge, MA, USA, 1962.
- [2] A. Viterbi and J. Omura, “Trellis encoding of memoryless discrete-time sources with a fidelity criterion,” *IEEE Trans. Inf. Theory*, vol. IT-20, no. 3, pp. 325–332, May 1974.
- [3] M. W. Marcellin and T. R. Fischer, “Trellis coded quantization of memoryless and Gauss–Markov sources,” *IEEE Trans. Commun.*, vol. 38, no. 1, pp. 82–93, Jan. 1990.
- [4] J. Garcia-Frias and Y. Zhao, “Compression of binary memoryless sources using punctured turbo codes,” *IEEE Commun. Lett.*, vol. 6, no. 9, pp. 394–396, Sep. 2002.
- [5] Y. Matsunaga and H. Yamamoto, “A coding theorem for lossy data compression by LDPC codes,” *IEEE Trans. Inf. Theory*, vol. 49, no. 9, pp. 2225–2229, Sep. 2003.
- [6] N. Hussami, S. B. Korada, and R. Urbanke, “Performance of polar codes for channel and source coding,” in *Proc. IEEE Int. Symp. Inf. Theory*, Jun./Jul. 2009, pp. 1488–1492.
- [7] M. Karzand and E. Telatar, “Polar codes for q-ary source coding,” in *Proc. IEEE Int. Symp. Inf. Theory*, Jun. 2010, pp. 909–912.
- [8] S. B. Korada and R. L. Urbanke, “Polar codes are optimal for lossy source coding,” *IEEE Trans. Inf. Theory*, vol. 56, no. 4, pp. 1751–1768, Apr. 2010.
- [9] M. Wainwright and E. Martinian, “Low-density graph codes that are optimal for binning and coding with side information,” *IEEE Trans. Inf. Theory*, vol. 55, no. 3, pp. 1061–1079, Mar. 2009.
- [10] M. J. Wainwright, E. Maneva, and E. Martinian, “Lossy source compression using low-density generator matrix codes: Analysis and algorithms,” *IEEE Trans. Inf. Theory*, vol. 56, no. 3, pp. 1351–1368, Mar. 2010.
- [11] A. G. Dimakis, M. J. Wainwright, and K. Ramchandran, “Lower bounds on the rate-distortion function of LDGM codes,” in *Proc. IEEE Inf. Theory Workshop*, Sep. 2007, pp. 650–655.
- [12] S. Kudekar and R. Urbanke, “Lower bounds on the rate-distortion function of individual LDGM codes,” in *Proc. Int. Symp. Turbo Codes Related Topics*, Sep. 2008, pp. 379–384.
- [13] F. Krzakala, A. Montanari, F. Ricci-Tersenghi, G. Semerjian, and L. Zdeborová, “Gibbs states and the set of solutions of random constraint satisfaction problems,” *Proc. Nat. Acad. Sci. USA*, vol. 104, no. 25, pp. 10318–10323, 2007.
- [14] N. Noorshams and M. Wainwright, “Lossy source coding with sparse graph codes: A variational formulation of soft decimation,” in *Proc. 48th Annu. Allerton Conf. Commun., Control, Comput.*, Sep./Oct. 2010, pp. 354–360.
- [15] T. Murayama, “Thouless-Anderson-Palmer approach for lossy compression,” *Phys. Rev. E, Stat. Phys. Plasmas Fluids Relat. Interdiscip. Top.*, vol. 69, no. 3, p. 035105, 2004.
- [16] M. J. Wainwright and E. Maneva, “Lossy source encoding via message-passing and decimation over generalized codewords of LDGM codes,” in *Proc. IEEE Int. Symp. Inf. Theory*, Adelaide, SA, Australia, Sep. 2005, pp. 1493–1497.
- [17] S. Ciliberti, M. Mézard, and R. Zecchina, “Message-passing algorithms for non-linear nodes and data compression,” *Complexus*, vol. 3, no. 58, pp. 58–65, Aug. 2006.
- [18] S. Ciliberti and M. Mézard, “The theoretical capacity of the parity source coder,” *J. Stat. Mech., Theory Exp.*, vol. 2005, Oct. 2005, Art. no. P10003.
- [19] A. Montanari, F. Ricci-Tersenghi, and G. Semerjian, “Solving constraint satisfaction problems through belief propagation-guided decimation,” in *Proc. 45th Annu. Allerton Conf. Commun., Control, Comput.*, Monticello, IL, USA, Sep. 2007, pp. 352–359.
- [20] A. Coja-Oghlan, “A better algorithm for random  $k$ -SAT,” *SIAM J. Comput.*, vol. 39, no. 7, pp. 2823–2864, 2010.
- [21] E. Martinian and J. S. Yedidia, “Iterative quantization using codes on graphs,” in *Proc. Allerton Conf. Commun., Control, Comput.*, Monticello, IL, USA, Oct. 2003, pp. 110–122.
- [22] G. Demay, V. Rathi, and L. K. Rasmussen, “Optimality of LDGM-LDPC compound codes for lossy compression of binary erasure source,” in *Proc. Int. Symp. Inf. Theory Appl. (ISITA)*, Oct. 2010, pp. 589–594.
- [23] G. Demay, V. Rathi, and L. K. Rasmussen, “Rate distortion bounds for binary erasure source using sparse graph codes,” in *Proc. Data Compress. Conf.*, Mar. 2010, pp. 49–58.
- [24] T. Filler and J. Fridrich, “Binary quantization using belief propagation with decimation over factor graphs of LDGM codes,” in *Proc. 45th Annu. Allerton Conf. Commun., Control, Comput.*, Monticello, IL, USA, Sep. 2007, pp. 495–501.
- [25] D. Castanheira and A. Gameiro, “Lossy source coding using belief propagation and soft-decimation over LDGM codes,” in *Proc. IEEE Int. Symp. Pers., Indoor Mobile Radio Commun.*, Istanbul, Turkey, Sep. 2010, pp. 431–436.
- [26] V. Aref, N. Macris, and M. Vuffray, “Approaching the rate-distortion limit with spatial coupling, belief propagation, and decimation,” *IEEE Trans. Inf. Theory*, vol. 61, no. 7, pp. 3954–3979, Jul. 2015.
- [27] V. Aref, N. Macris, R. Urbanke, and M. Vuffray, “Lossy source coding via spatially coupled LDGM ensembles,” in *Proc. IEEE Int. Symp. Inf. Theory (ISIT)*, Jul. 2012, pp. 373–377.

- [28] D. Divsalar, S. Dolinar, C. R. Jones, and K. Andrews, "Capacity-approaching protograph codes," *IEEE J. Sel. Areas Commun.*, vol. 27, no. 6, pp. 876–888, Aug. 2009.
- [29] T. Berger and J. D. Gibson, "Lossy source coding," *IEEE Trans. Inf. Theory*, vol. 44, no. 6, pp. 2693–2723, Oct. 1998.
- [30] T. M. Cover and J. A. Thomas, *Elements of Information Theory*. Hoboken, NJ, USA: Wiley, 2012.
- [31] J. Thorpe, "Low-density parity-check LDPC codes constructed from protographs," Jet Propuls. Lab., Pasadena, CA, USA, Tech. Rep. 42-154, Aug. 2003.
- [32] D. G. M. Mitchell, M. Lentmaier, and D. J. Costello, "Spatially coupled LDPC codes constructed from protographs," *IEEE Trans. Inf. Theory*, vol. 61, no. 9, pp. 4866–4889, Sep. 2015.
- [33] A. R. Iyengar, M. Papaleo, P. H. Siegel, J. K. Wolf, A. Vanelli-Coralli, and G. E. Corazza, "Windowed decoding of protograph-based LDPC convolutional codes over erasure channels," *IEEE Trans. Inf. Theory*, vol. 58, no. 4, pp. 2303–2320, Apr. 2012.
- [34] W. E. Ryan and S. Lin, *Channel Codes: Classical and Modern*. New York, NY, USA: Cambridge Univ. Press, 2009.



**Ahmad Golmohammadi** received the M.S. degree in electrical engineering from the University of Southern California, Los Angeles, USA, in 2012. He is currently pursuing the Ph.D. degree with the Klipsch School of Electrical and Computer Engineering Department, New Mexico State University, Las Cruces, NM, USA. His research interests include coding theory, information theory, and signal processing.



**David G. M. Mitchell** (S'08–M'09–SM'16) received the Ph.D. degree in electrical engineering from the University of Edinburgh, U.K., in 2009. From 2009 to 2015, he held a Post-Doctoral Research Associate and Visiting Assistant Professor positions with the Department of Electrical Engineering, University of Notre Dame, USA. Since 2015, he has been an Assistant Professor with the Klipsch School of Electrical and Computer Engineering, New Mexico State University, USA. His research interests are in the area of digital communications, with emphasis on error control coding and information theory.



**Jörg Kliewer** (S'97–M'99–SM'04) received the Dipl.Ing. (M.Sc.) degree in electrical engineering from the Hamburg University of Technology, Hamburg, Germany, in 1993, and the Dr. Ing. degree (Ph.D.) in electrical engineering from the University of Kiel, Germany, in 1999, respectively.

From 1993 to 1998, he was a Research Assistant with the University of Kiel, where he was a Senior Researcher and a Lecturer from 1999 to 2004. In 2004, he visited the University of Southampton, U.K., for one year, and from 2005 to 2007, he was with the University of Notre Dame, Notre Dame, IN, USA, as a Visiting Assistant Professor. From 2007 to 2013, he was with New Mexico State University, Las Cruces, NM, USA. Since 2014, he has been with the New Jersey Institute of Technology, Newark, NJ, USA, as an Associate Professor, and since August 2018, as a Professor. His research interests span information and coding theory, graphical models, and statistical algorithms, which includes applications to networked communication and security, data storage, and biology.

Dr. Kliewer has been a member of the Editorial Board of the *IEEE Information Theory Newsletter* since 2012. He was a recipient of the Leverhulme Trust Award in 2003 and the German Research Foundation Fellowship Award in 2004. He was an Associate Editor of the *IEEE TRANSACTIONS ON COMMUNICATIONS* from 2008 to 2014, and since 2015, he has been serving as an Area Editor for the same journal. He has also been an Associate Editor of the *IEEE TRANSACTIONS ON INFORMATION THEORY* since 2017.



**Daniel J. Costello, Jr.** (S'62–M'69–SM'78–F'85–LF'08) was born in Seattle, WA, USA, in 1942. He received the B.S.E.E. degree from Seattle University, Seattle, WA, USA, in 1964, and the M.S. and Ph.D. degrees in electrical engineering from the University of Notre Dame, Notre Dame, IN, USA, in 1966 and 1969, respectively. He joined the Faculty of the Illinois Institute of Technology, Chicago, IL, USA, in 1969. In 1985, he became a Professor of electrical engineering with the University of Notre Dame, and from 1989 to 1998, he served as the Chair of the

Department of Electrical Engineering. In 1991, he was selected as one of 100 Seattle University alumni to receive the Centennial Alumni Award in recognition of alumni who have displayed outstanding service to others, exceptional leadership, or uncommon achievement. In 1999, he received a Humboldt Research Prize from the Alexander von Humboldt Foundation in Germany. In 2000, he was named the Leonard Bettex Professor of Electrical Engineering at Notre Dame, and in 2009 he became Bettex Professor Emeritus.

Dr. Costello was elected an IEEE Fellow in 1985. He served 18 years as a member of the Information Theory Society Board of Governors, and in 1986, he was President of the BOG. In 2000, the IEEE Information Theory Society selected him as a recipient of a Third-Millennium Medal. In 2009, he was a co-recipient of the IEEE Donald G. Fink Prize Paper Award, which recognizes an outstanding survey, review, or tutorial paper in any IEEE publication issued during the previous calendar year. In 2012, he was a co-recipient of the joint IEEE Information Theory Society/Communications Society Prize Paper Award, which recognizes an outstanding research paper in the IT or COM Transactions during the previous two calendar years. In 2013, he received the Aaron D. Wyner Distinguished Service Award from the IEEE Information Theory Society, which recognizes outstanding leadership in and long standing exceptional service to the information theory community. In 2014, he received the IEEE Educational Activities Board Vice President's Recognition Award. In 2015, he received the IEEE Leon K. Kirchner Graduate Teaching Award, which recognizes inspirational teaching of graduate students in the IEEE fields of interest.

His research interests are in digital communications, with special emphasis on error control coding and coded modulation. He has numerous technical publications in his field, and in 1983 he co-authored a textbook *Error Control Coding: Fundamentals and Applications*, the 2nd edition of which was published in 2004.